Tip-surface forces, amplitude, and energy dissipation in amplitude-modulation (tapping mode) force microscopy

Álvaro San Paulo and Ricardo García*

Instituto de Microelectrónica de Madrid, CSIC, Isaac Newton 8, 28760 Tres Cantos, Madrid, Spain

Amplitude-modulation (tapping mode) atomic force microscopy is a technique for high resolution imaging of a wide variety of surfaces in air and liquid environments. Here by using the virial theorem and energy conservation principles we have derived analytical relationships between the oscillation amplitude, phase shift, and average tip-surface forces. We find that the average value of the interaction force and oscillation and the average power dissipated by the tip-surface interaction are the quantities that control the amplitude reduction. The agreement obtained between analytical and numerical results supports the analytical method.

Amplitude-modulation force microscopy, usually known as tapping mode AFM is the most extensively used dynamic force microscopy method for nanometer-scale characterization and modification of surfaces in air and liquid environments. High resolution images of protein membranes,[1] isolated proteins,[2] and polymers[3] have been obtained as well as *true* atomic resolution images of inorganic surfaces.[4] In amplitude-modulation force microscopy the tip is excited at a frequency close to its resonance value with a free oscillation amplitude ranging between 5 and 100 nm. The tip-cantilever ensemble is approached towards the sample until the oscillation amplitude reaches a set point value. An image is formed by scanning the tip across the sample while the amplitude is kept at a set point value.

The experimental results have prompted a series of theoretical studies aiming to provide a framework to understand the tip motion under the influence of an interaction potential.[5–12] However, the theoretical analysis of large amplitude dynamic AFM is not straightforward. The force gradient may change considerably during an oscillation, which compromises the use of harmonic approximations.[13] On the other hand, the tip-surface force contains nonlinear terms which may introduce nonlinear features in the dynamics of the tip motion.[14] Furthermore, dissipative processes such as surface adhesion hysteresis, viscoelasticity or electronic dissipation may also be involved. As a consequence most theoretical studies have involved some kind of numerical simulations. They have established the existence of two different interaction regimes, *attractive* and *repulsive*. In the attractive regime, a negative average interaction force dominates the amplitude reduction while in the repulsive regime, the average interaction force is repulsive.[11]

In this paper we apply energy conservation principles and the virial theorem to derive analytical expressions to describe the amplitude and phase shift dependencies with the average value of the interaction force and oscillation and the average power dissipated by the tip-sample interaction. These expressions have been applied to study amplitude curves that show a continuous transition between the attractive and repulsive interaction regimes. We also discuss the operation of amplitude-modulation AFM for a tip-surface interaction dominated by long range attractive van der Waals forces.

The dynamics of the tip motion in amplitude-modulation AFM can be approximately described by the differential equation

$$m\ddot{z} = -k_c z - \frac{m\omega_0}{Q}\dot{z} + F_{ts} + F_0 \cos(\omega t). \qquad (1)$$

The total force that governs the tip motion includes the elastic response of the cantilever, the hydrodynamic damping with the medium, the tip-sample interaction force and the periodic driving force. Q, k_c, and ω_0 are the quality factor, spring constant, and angular resonance frequency of the free cantilever, respectively. F_0 and ω are the amplitude and angular frequency of the driving force. The approximations used to derive Eq. (1) as well as their justification can be found elsewhere.[11]

The steady-state oscillation can be approximated by a sinusoidal oscillation,

$$z(z_c,t) = z_0(z_c) + A(z_c)\cos[\omega t - \phi(z_c)], \qquad (2)$$

where z_0, A, and ϕ are the mean deflection, amplitude, and phase shift of the oscillation, respectively. We denote z_c as the equilibrium tip-sample separation in absence of interactions. The above approximation has been applied successfully by several authors. Wang found a good agreement between theoretical and experimental amplitude versus frequency curves on a polyethylene sample.[9] Quantitative agreement between phase shifts and energy dissipation measurements on biological membranes was also obtained by Tamayo and García.[15] Using an impact model for the tip-sample interaction Salapaka *et al.* found that for standard operating conditions the tip evolves into a stable periodic orbit with a period equal to the period of the forcing.[16]

According to the virial theorem the time averaged kinetic energy of the tip is equal to its virial,[17]

$$\langle K \rangle = \tfrac{1}{2} m\langle \dot{z}^2 \rangle = -\tfrac{1}{2} \langle F \cdot z \rangle. \qquad (3)$$

The combination of Eqs. (1), (2), and (3) yields the following relationship:

$$\cos\phi = \frac{2Q}{k_c A A_0}\left[\frac{\langle F_{ts}\rangle^2}{k_c} - \langle F_{ts}\cdot z\rangle + \frac{1}{2}k_c A^2\left(1 - \frac{\omega^2}{\omega_0^2}\right)\right], \qquad (4)$$

64 193411-1

where $A_0 = QF_0/k_c$ is the free oscillation amplitude and $\langle F_{ts} \rangle = (1/T) \oint F_{ts} dt$.

On the other hand, it can be shown that

$$\langle F_{ts} \rangle = k_c \langle z \rangle = k_c z_0. \tag{5}$$

In many experimental situations, the mean deflection z_0 is negligible compared to the oscillation amplitude A. Then, $A \gg z_0$ in combination with Eq. (5) implies

$$\frac{\langle F_{ts} \rangle^2}{k_c} = \langle F_{ts} \rangle \cdot z_0 \ll \langle F_{ts} \cdot z \rangle. \tag{6}$$

The above approximations and $\omega = \omega_0$ turn Eq. (4) into

$$\cos \phi \approx -\frac{2Q \langle F_{ts} \cdot z \rangle}{k_c A A_0}. \tag{7}$$

An additional relationship between A, ϕ, and the tip-sample interaction force is obtained by assuming that the external excitation coincides with the energy dissipated in the oscillation[15,18]

$$\sin \phi \approx \frac{A \omega}{A_0 \omega_0} + \frac{2Q P_{ts}}{k_c A A_0 \omega}, \tag{8}$$

where $P_{ts} = \langle F_{ts} \cdot \dot{z} \rangle$ is the power dissipated by the tip-sample interaction.

The combination of Eqs. (7) and (8) gives a relationship between the amplitude, $\langle F_{ts} \cdot z \rangle$ and P_{ts}

$$A \approx \frac{A_0}{\sqrt{2}} \left(1 - \frac{2P_{ts}}{P_{med}} \pm \sqrt{1 - \frac{4P_{ts}}{P_{med}} - 16 \left(\frac{\langle F_{ts} \cdot z \rangle}{F_0 A_0} \right)^2} \right)^{1/2}, \tag{9}$$

where P_{med} is the power dissipated by hydrodynamic damping

$$P_{med} = \frac{\omega_0 k_c A_0^2}{2Q}. \tag{10}$$

The positive sign of the square root in Eq. (9) corresponds to $A/A_0 > (1/2 - P_{ts}/P_{med})^{1/2}$, while the negative sign corresponds to $A/A_0 < (1/2 - P_{ts}/P_{med})^{1/2}$.

Equation (9) can be simplified for conservative interactions ($P_{ts} = 0$) or negligible tip-sample power dissipation ($P_{ts} \ll P_{med}$),

$$A \approx \frac{A_0}{\sqrt{2}} \left(1 \pm \sqrt{1 - 16 \left(\frac{\langle F_{ts} \cdot z \rangle}{F_0 A_0} \right)^2} \right)^{1/2}. \tag{11}$$

For oscillations with small contact times ($\sim 0.2\ T$ or less) it can be shown that

$$\langle F_{ts} \cdot z \rangle \approx -A \langle F_{ts} \rangle. \tag{12}$$

Small contact times and conservative interactions allow one to express the phase shift as

$$\cos \phi \approx 2 \frac{\langle F_{ts} \rangle}{F_0}, \tag{13}$$
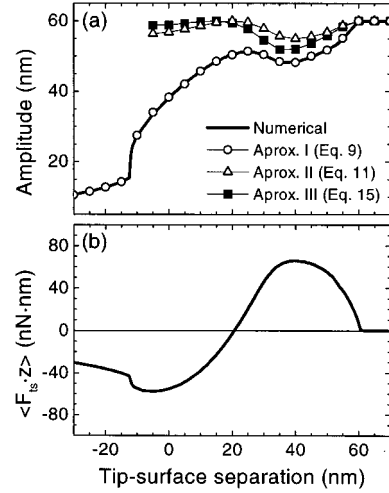

FIG. 1. (a) Amplitude curve for a compliant and viscoelastic material. The solid line represents the numerical simulation while the symbols correspond to the different analytical expressions. (b) Numerical determination of $\langle F_{ts} \cdot z \rangle$.

$$\sin \phi = \frac{A}{A_0}. \tag{14}$$

Finally, the combination of Eqs. (13) and (14) gives

$$A \approx A_0 \left(1 - 4 \left(\frac{\langle F_{ts} \rangle}{F_0} \right)^2 \right)^{1/2}. \tag{15}$$

The amplitude and $\cos \phi$ dependence on $\langle F_{ts} \cdot z \rangle$ are reminiscent of the relationship found by Giessibl[19] to describe frequency shifts in frequency modulation AFM. Based on the Harmonic-Jacobi formalism it was found that the shift in the resonance frequency was $\Delta f \propto \langle F_{ts} \cdot z \rangle$. This points out the close relationship between frequency and amplitude-modulation AFM modes.

Numerical calculations have extensively been used to simulate the tip motion in amplitude-modulation AFM. To establish their range of applicability, the above expressions are compared with numerical simulations. For a given tip-surface interaction force the quantities $\langle F_{ts} \rangle$, $\langle F_{ts} \cdot z \rangle$ and P_{ts} are obtained by numerical integration. Those values are introduced in the corresponding expressions for the amplitude and phase shift. The results obtained by the application of the analytical approximations are compared with those obtained independently by direct numerical integration of the motion equation.

Figure 1 shows the amplitude as a function of the tip-surface distance for a compliant and viscoelastic material. The solid line represents the numerical solution while the symbols are the results obtained with the different equations. The tip-surface interaction force includes long-range attractive van der Waals force and short-range repulsive forces given by the JKR contact mechanics.[20] The values used for the resonance frequency, spring constant and quality factor of the cantilever are $f_0 = \omega_0/2\pi = 350$ kHz, $k_c = 40$ nm, and $Q = 400$, respectively. The sample is characterized by a
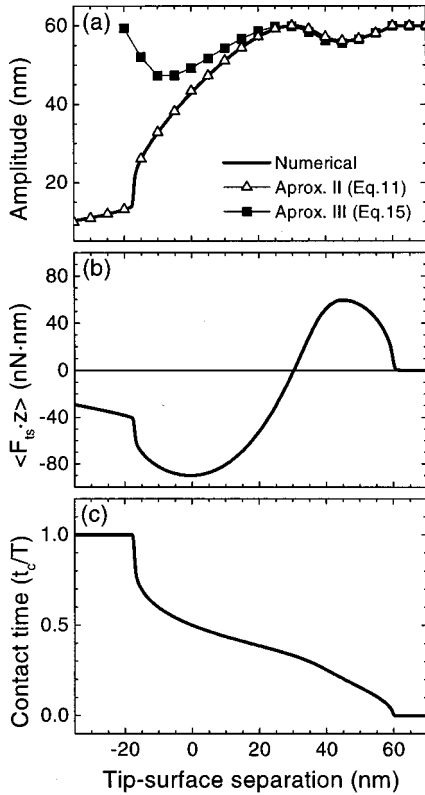
FIG. 2. (a) Amplitude curve for a compliant and elastic material. The solid line represents the numerical simulation while the symbols correspond to the different analytical expressions. (b) Numerical determination of $\langle F_{ts} \cdot z \rangle$. (c) Tip-sample contact time.

Young's modulus of 7 MPa, surface energy of 30 mJ/m^2, viscosity η of 1 Pa·s and a Hamaker constant of 6.16 $\times 10^{20}$ J. The tip radius is $R = 30$ nm and the free amplitude is $A_0 = 60$ nm.

An excellent agreement is obtained between Eq. (9) and the numerical solution. In both cases the amplitude curves show a local minimum and a local maximum. These local extremes are a consequence of the competition between attractive and repulsive forces to control the amplitude reduction. Mathematically the minimum is related to the existence of a maximum in the quantity $\langle F_{ts} \cdot z \rangle$ [Fig. 1(b)]. The local maximum happens when the argument of the square root in Eq. (9) achieves a maximum. For the parameters used here it approximately coincides with $\langle F_{ts} \cdot z \rangle = 0$. The discrepancies observed when Eqs. (11) and (15) are used are not surprising due to the conservative character of the interactions considered in both equations.

Figure 2(a) shows the amplitude curve for the same system when inelastic processes are not allowed ($\eta = 0$ Pa·s). Excellent agreements are obtained among numerical simulations and Eqs. (9) and (11). The amplitude curve shows local extremes. Here the maximum reaches the free oscillation amplitude. This result is related to the absence of tip-sample inelastic interactions. Equation (11) allows us to associate the local minimum to a maximum in the dependence of $\langle F_{ts} \cdot z \rangle$ on separation. The maximum happens when $\langle F_{ts} \cdot z \rangle = 0$. On the other hand, Eq. (15) does not reproduce the observed amplitude curve (numerical solution) because the
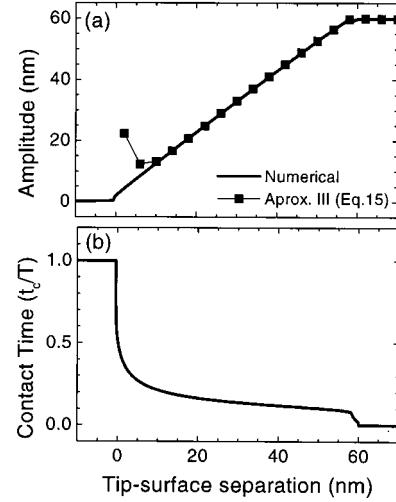

FIG. 3. (a) Amplitude curve for a stiff and elastic material. Solid line is the numerical simulation while the symbols have been obtained by Eq. (15). (b) Tip-sample contact time.

contact time is a sizeable fraction of the oscillation period [Fig. 2(b)].

For the same external parameters the contact time decreases with the stiffness of the sample.[6] Then, good agreements could be expected between numerical simulations and Eq. (15) for stiff materials. Figure 3(a) shows the amplitude curve for a material with $E = 1$ GPa and no viscosity. The agreement is excellent except for very small tip-surface separations where the contact time shows a sharp increase [Fig. 3(b)]. In this case the DMT contact mechanics[21] was used to model the tip-surface repulsive forces (see Ref. 22 for discussion about the use of contact mechanics models in AFM).

It has been previously demonstrated the existence of steady state oscillations that do not involve tip-surface contact.[23–25] Assuming a sphere-plane geometry, the average value of the van der Waals force and oscillation can be calculated analytically,

$$\langle F_{vdW} \cdot z \rangle = \frac{1}{T} \oint \frac{-HRz}{6(z_c + z)^2} dt = \frac{HR}{6A} \left[\left(\frac{z_c}{A} \right)^2 - 1 \right]^{-3/2}. \tag{16}$$

The combination of Eqs. (16) and (11) gives a relationship between the amplitude and the equilibrium tip-surface separation

$$\frac{z_c}{A_0} \approx \frac{A}{A_0} \left[1 + C \left(\left(\frac{A}{A_0} \right)^4 - \left(\frac{A}{A_0} \right)^6 \right)^{-1/3} \right]^{1/2}, \tag{17}$$

where C is a dimensionless parameter given by

$$C = \left(\frac{HR}{3F_0 A_0^2} \right)^{2/3}. \tag{18}$$

Since F_0 is the maximum of the driving force, the term $F_0 A_0^2$ can be related to the strength of the driving force while HR can be related to the strength of the attractive interaction. For a given tip geometry and Hamaker constant, high values of C correspond to a high van der Waals interaction relative
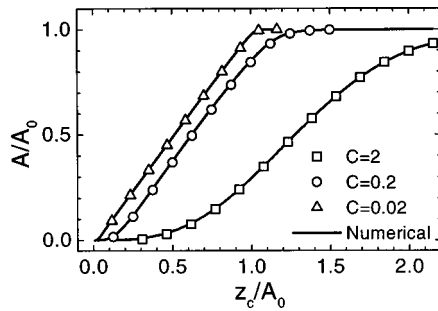
FIG. 4. Reduced amplitude versus reduced tip-surface separation for a tip oscillating without tip-surface mechanical contact.

to the driving force. C ranges between 10 and 10^{-4} for common experimental conditions, $k_c \in [20-50]$ N/m, $H \sim 10^{-19}$ J, $R \in [5-50]$ nm, $Q = 400$, and $A_0 \in [1-20]$ nm.

Amplitude vs distance curves for $C = 2$, $C = 0.2$, and $C = 0.02$ are shown in Fig. 4. The above values of C correspond to $A_0 = 1.3$ nm, 4 nm, and 12 nm, respectively [parameters as in Fig. (1)]. The symbols are the results obtained by Eq. (17) while the numerical simulations are shown by solid lines. The agreement obtained between the above equation and the numerical results is excellent.

The amplitude curve for $C = 0.02$ shows an abrupt change of slope at $z_c = A_0$. For smaller separations, the slope takes a constant value very close to unity. On the other hand, the slope of the amplitude curve for $C = 0.2$ varies smoothly from zero at large separations to unity at intermediate separations, and then back to zero at small separations. The nonlinear dependence of the amplitude on tip-surface average distance is more evident for higher values of C (see curve for $C = 2$).

Equation (17) also suggests a procedure to determine the values of the Hamaker constant. This requires the measurement of amplitude curves, then Eq. (17) could be used to

determine the C value that produces the best fit to the experimental curve. The last step involves the use of Eq. (18) to deduce the Hamaker constant.

In summary, we have deduced several analytical expressions to study the tip motion in amplitude-modulation atomic force microscopy. Those expressions have been derived by the application of the virial theorem and energy conservation principles. Direct comparisons between numerical and analytical results have confirmed the validity of the analytical approach. The analytical approach states that the average interaction force times the deflection and the tip-sample energy dissipation are the quantities that control the amplitude reduction. The dependence on average quantities is a direct consequence of a tip motion that experiences different values of the tip-surface force per cycle.

Those expressions have been applied to study smooth transitions between attractive and repulsive interaction regimes. Those transitions are characterized by the presence of a local maximum in amplitude curves. In the absence of inelastic interactions the local maximum coincides with the value of the free oscillation amplitude. This rather surprising result emphasizes the simultaneous contribution of attractive and repulsive forces to the tip motion.

For a van der Waals interaction a relationship is obtained between the oscillation amplitude and the tip-surface separation. This relationship is parametrized by the ratio of the strengths of attractive and external driving forces. For small ratios a one to one correspondence between the amplitude and average tip-surface separation is found. The above expression also suggests a new method to determine the Hamaker constant.

---

*Corresponding author. Email address: rgarcia@imm.cnm.csic.es

[1] C. Möller, M. Allen, V. Elings, A. Engel, and D. Müller, Biophys. J. **77**, 1150 (1999).

[2] A. San Paulo and R. García, Biophys. J. **78**, 1599 (2000).

[3] G. Bar, Y. Thomann, and M.-H. Whangbo, Langmuir **14**, 1219 (1998).

[4] F. Ohnesorge, Surf. Interface Anal. **27**, 379 (1999).

[5] J. Chen *et al.*, Nanotechnology **5**, 199 (1994).

[6] J. Tamayo and R. García, Langmuir **12**, 4430 (1996).

[7] B. Anczykowski, D. Krüger, and H. Fuchs, Phys. Rev. B **53**, 15485 (1996).

[8] A. Kühle, A. H. Soerensen, and J. Bohr, J. Appl. Phys. **81**, 6562 (1997).

[9] L. Wang, Appl. Phys. Lett. **73**, 3781 (1998).

[10] L. Nony, R. Boisgard, and J. P. Aimé, J. Chem. Phys. **111**, 1615 (1999).

[11] R. García and A. San Paulo, Phys. Rev. B **60**, 4961 (1999).

[12] X. Chen *et al.*, Surf. Sci. **460**, 292 (2000).

[13] H. Hölsher, U. D. Schwarz, and R. Weisendanger, Appl. Surf. Sci. **140**, 344 (1999).

[14] R. García and A. San Paulo, Phys. Rev. B **61**, R13381 (2000).

[15] J. Tamayo and R. García, Appl. Phys. Lett. **73**, 2926 (1998).

[16] M. V. Salapaka, D. J. Chen, and J. P. Cleveland, Phys. Rev. B **61**, 1106 (2000).

[17] H. Goldstein, *Classical Mechanics* (Addison-Wesley, Reading, MA, 1981).

[18] J. P. Cleveland *et al.*, Appl. Phys. Lett. **72**, 2613 (1998).

[19] F. Giessibl, Phys. Rev. B **56**, 16010 (1997).

[20] K. L. Johnson, K. Kendall, and A. D. Roberts, Proc. R. Soc. London, Ser. A **324**, 301 (1971).

[21] B. V. Derjaguin, V. M. Muller, and Y. P. Toporov, J. Colloid Interface Sci. **53**, 314 (1975).

[22] W. N. Unertl, J. Vac. Sci. Technol. A **17**, 1779 (1999).

[23] R. García and A. San Paulo, Ultramicroscopy **82**, 79 (2000).

[24] P. J. de Pablo *et al.*, Phys. Rev. B **61**, 14179 (2000).

[25] G. Haugstad and R. Jones, Ultramicroscopy **76**, 77 (1999).